The Astrophysical Journal, 645:464–469, 2006 July 1

SWIFT OBSERVATIONS OF GRB 050603: AN AFTERGLOW WITH A STEEP LATE-TIME DECAY SLOPE

Dirk Grupe,[1] Peter J. Brown,[1] Jay Cummings,[2] Bing Zhang,[3] Alon Retter,[1] David N. Burrows,[1] Patricia T. Boyd,[2] Milvia Capalbi,[4] Neil Gehrels,[2] Stephen T. Holland,[2,5] Peter Mészáros,[1,6] John A. Nousek,[1] Jamie A. Kennea,[1] Paul O'Brien,[7] Julian Osborne,[7] Claudio Pagani,[1] Judith L. Racusin,[1] Peter Roming,[1] and Patricia Schady[1,8]

Received 2005 December 13; accepted 2006 March 15

ABSTRACT

We report the results of *Swift* observations of the gamma-ray burst GRB 050603. With a V magnitude $V = 18.2$ about 10 hr after the burst, the optical afterglow was the brightest thus far detected by *Swift* and one of the brightest optical afterglows ever seen. The Burst Alert Telescope (BAT) light curves show three fast-rise exponential-decay spikes with $T_{90} = 12$ s and a fluence of 7.6×10^{-6} ergs cm^{-2} in the 15–150 keV band. With $E_{\gamma,\mathrm{iso}} = 1.26 \times 10^{54}$ ergs, it was also one of the most energetic bursts of all times. The *Swift* spacecraft began observation of the afterglow with the narrow-field instruments about 10 hr after the detection of the burst. The burst was bright enough to be detected by the *Swift* UV/Optical telescope (UVOT) for almost 3 days and by the X-Ray Telescope (XRT) for a week after the burst. The X-ray light curve shows a rapidly fading afterglow with a decay index $\alpha = 1.76^{+0.15}_{-0.07}$. The X-ray energy spectral index was $\beta_X = 0.71 \pm 0.10$ with the column density in agreement with the Galactic value. The spectral analysis does not show an obvious change in the X-ray spectral slope over time. The optical UVOT light curve decays with a slope of $\alpha = 1.8 \pm 0.2$. The steepness and the similarity of the optical and X-ray decay rates suggest that the afterglow was observed after the jet break. We estimate a jet opening angle of about 1°–2°.

Subject heading: gamma rays: bursts

Online material: color figures

1. INTRODUCTION

With an isotropic equivalent energy release on the order of 10^{52}–10^{54} ergs, gamma-ray bursts (GRBs) are among the most energetic events in the universe besides the big bang. GRBs can be separated into two classes: short and long bursts. Long bursts, with durations longer than 2 s (e.g., Kouveliotou et al. 1993), are associated with the collapse of a very massive star and the formation of a black hole (Woosley 1993). Short bursts are thought to be the result of a neutron star (NS)–NS or NS–black hole merger (e.g., Eichler et al. 1989; Paczyński 1991). The leading theoretical model for GRBs and their afterglows is the fireball model (see Mészáros & Rees 1997; Sari et al. 1998; Zhang & Mészáros 2004 and references within), in which the GRB is produced by internal shocks in a relativistic fireball, while the afterglow is produced in external shocks that are created when the fireball encounters the ambient external medium.

The multiwavelength mission *Swift* (Gehrels et al. 2004) was launched on 2004 November 20 in order to hunt for GRBs. It is in low-Earth orbit at an altitude of 600 km s^{-1}. The *Swift* observatory is equipped with three telescopes: (1) the Burst Alert Telescope (BAT; Barthelmy 2005), (2) the X-Ray Telescope (XRT; Burrows et al. 2005), and (3) the UV-Optical Telescope (UVOT; Roming et al. 2005a). BAT is a coded mask experiment and operates in the 15–350 keV energy range. The XRT detector is a copy of the MOS CCDs used on board *XMM-Newton* (Turner et al. 2001). It operates between 0.3 and 10 keV in three observing modes, photon counting (PC), which is equivalent to the full-frame mode on *XMM-Newton*, windowed timing (WT), and low-rate photodiode mode (LRPD), which is only used for extremely bright sources (Hill et al. 2004). The UVOT is a sister instrument to *XMM-Newton*'s Optical Monitor (OM; Mason et al. 2001) and includes a similar set of filters to the OM (Mason et al. 2001; Roming et al. 2005a).

As reported by Nousek et al. (2006), *Swift* has observed a general behavior of GRB afterglow X-ray light curves: a fast decay with slope α_1 in the first 100 s is followed by a much shallower decay slope α_2. This continues over a span of several thousands of seconds after the burst and is followed by a steeper decay slope α_3 (see also Zhang et al. 2006). The mean decay slopes of the 27 afterglows discussed in Nousek et al. (2006) are $\alpha_1 = 3.38 \pm 1.27$, $\alpha_2 = 0.76 \pm 0.34$, and $\alpha_3 = 1.33 \pm 0.32$.

In this paper we report the *Swift* observations of GRB 050603. The paper is organized as follows: In § 2 we describe the observations and the data reduction and analysis; in § 3 we present the results, which are then discussed in § 4. Throughout the paper decay and energy spectral indices α and β are defined as $F_\nu(t, \nu) \propto (t - t_0)^{-\alpha}\nu^{-\beta}$ with t_0 the trigger time of the burst. Luminosities are calculated assuming a ΛCDM cosmology with $\Omega_M = 0.27$, $\Omega_\Lambda = 0.73$, and a Hubble constant of $H_0 = 71$ km s^{-1} Mpc^{-1} using the luminosity distances given by Hogg (1999). All errors are 1 σ unless stated otherwise.

2. OBSERVATIONS AND DATA REDUCTION

GRB 050603 was detected by the BAT on 2005 June 3 at 06:29:05 UT (Retter et al. 2005) with the trigger ID 131560. Due to engineering tests of the *Swift* satellite, the narrow-field

[1] Department of Astronomy and Astrophysics, Pennsylvania State University, 525 Davey Lab, University Park, PA 16802.
[2] NASA Goddard Space Flight Center, Greenbelt, MD 20771.
[3] Department of Physics, University of Nevada, Las Vegas, NV 89154.
[4] ASI Science Data Center, via G. Galilei, I-00044 Frascati, Rome, Italy.
[5] Universities Space Research Association, Seabrook, MD 20706.
[6] Department of Physics, Pennsylvania State University, University Park, PA 16802.
[7] Department of Physics and Astronomy, University of Leicester, Leicester LE1 7R, UK.
[8] Mullard Space Science Laboratory, Holmbury St. Mary, Dorking, Surrey RH5 6NT, UK.

TABLE 1
LOG OF THE *Swift* XRT OBSERVATIONS OF GRB 050603

Segment	Start Time (UT)	Stop Time (UT)	T_{exp} (s)	Binning[a]
001	2005 Jun 03, 15:49:47	2005 Jun 03, 22:32:14	7122	50
002	2005 Jun 04, 00:02:16	2005 Jun 06, 21:10:00	72838	50
003	2005 Jun 07, 00:04:50	2005 Jun 07, 23:15:57	14612	25
004	2005 Jun 08, 00:26:48	2005 Jun 08, 23:22:58	11858	15
005	2005 Jun 09, 00:32:42	2005 Jun 09, 23:28:58	9840	10
006	2005 Jun 10, 00:39:43	2005 Jun 10, 23:35:57	11184	10
007	2005 Jun 11, 00:55:38	2005 Jun 11, 22:05:57	6463	UL[b]
008	2005 Jun 14, 20:23:42	2005 Jun 14, 23:59:56	3766	UL[b]
009	2005 Jun 15, 00:58:31	2005 Jun 15, 23:59:59	16453	UL[b]
010	2005 Jun 16, 00:04:59	2005 Jun 16, 23:59:57	11475	UL[b]
011	2005 Jun 17, 01:18:43	2005 Jun 17, 06:39:57	6292	UL[b]
012	2005 Jun 18, 00:05:01	2005 Jun 20, 23:03:20	44626	UL[b]
013	2005 Jun 24, 00:28:17	2005 Jun 24, 02:35:53	3284	UL[b]

[a] Number of photons per bin in the light curve.
[b] The source is not detected and only an upper limit can be given.

instruments UVOT and XRT were unable to observe the GRB afterglow until about 9.5 and 11 hr after the burst, respectively.

The UVOT began observing at 15:42:59 UT (Brown et al. 2005). The observations were made in the *V* filter with exposure time ratios of 1:8:1 per observing window so that the entire observation is not ruined if there is high background from the Earth limb at the beginning or end of the observation. Only the middle exposures were used, to eliminate the problems of high background. The NASA *Swift* Data Center (SDC)–processed sky images were astrometrically aligned with respect to an image of the field from the Digitized Sky Survey. Aperture photometry was performed using a $6''$ source aperture and a background annulus with inner and outer radii of $14''$ and $30''$, respectively. Once the afterglow in individual observations had fallen below 3 σ above background, they were co-added to bring the signal-to-noise ratio (S/N) above a 3 σ detection.

The GRB 050603 observations by the UVOT also revealed an infrequent problem in which the images do not contain events from the whole exposure time indicated in the header. Extension 4 of sequence 00131560001 reported an exposure time of 1500 s. However, a comparison of the count rate measured by the instrument and the counts in the image indicated that the image contained only 110 s of data. Thus, only 7.3% of the data were actually recorded. This resulted in an erroneous magnitude being reported in Brown et al. (2005), as pointed out by Berger (2005). We have corrected this by comparing the count rate as measured by the UVOT with the counts in the actual image to calculate the exposure time. When the header and calculated exposure times differed by more than 5%, the exposure keyword was changed to the calculated value. The software bug causing this problem was fixed on 2005 September 14; data taken before that date will be checked and corrected in the archive.

XRT started to take data at 17:19:27 UT (Racusin et al. 2005). GRB 050603 was observed over a period of about 2 weeks for a total of about 220 ks. The detailed observation log is listed in Table 1. All observations were performed in PC mode. The XRT data were reduced by the `xrtpipeline` version 0.9.9. Source photons were selected by XSELECT in a circular region with a radius of $r = 47''$ and the background photons in a circular region close by with a radius $r = 96''$. For the spectral data , events with grades 0–12 were selected with XSELECT. The spectral data were rebinned by `grppha` version 3.0.0, having at least a minimum of 20 photons per bin. The spectra were analyzed by XSPEC version 11.3.2. The auxiliary response files were created by `xrtmkarf` and the standard response matrix swxpc0to12_20010101v007.rmf was used.

Background-subtracted X-ray light curves in the 0.3–10.0 keV energy range were constructed using the ESO Munich Image Data Analysis Software MIDAS (ver. 04Sep). The binning was dynamically performed. At the beginning of the observations the binning was set to 50 photons bin^{-1}, while at later times it was reduced to 10 photons bin^{-1} as listed in Table 1. Also at later times the source extraction radius was reduced to 10 pixels (corresponding to $r = 23.''6$) in order to avoid confusion by the background. The X-ray light curve was fitted by power-law and broken power-law models in XSPEC. The count rates were

TABLE 2
CALCULATED POSITIONS OF GRB 050603

Position	R.A. (J2000.0)	Decl. (J2000.0)	Position Error (arcsec)	Reference
BAT on-board (BAT1)	02 39 55	−25 10 57	240	Retter et al. (2005)
BAT ground (BAT2)	02 39 56	−25 11 41	60	Fenimore et al. (2005)
XRT	02 39 56.73	−25 10 54.36	3.9	Moretti et al. (2005)
UVOT *V* filter	02 39 56.8	−25 10 54.9	1.0	Brown et al. (2005a)
Las Campanas *R* band	02 39 57	−25 10 54	0.5	Berger & McWilliam (2005)
VLA 8.5 GHz	02 39 56.9	−25 10 54.6	0.1	Cameron (2005)

NOTES.—Units of right ascension are hours, minutes, and seconds, and units of declination are degrees, arcminutes, and arcseconds. BAT1 and BAT2 refer to the positions as shown in Figure 1.

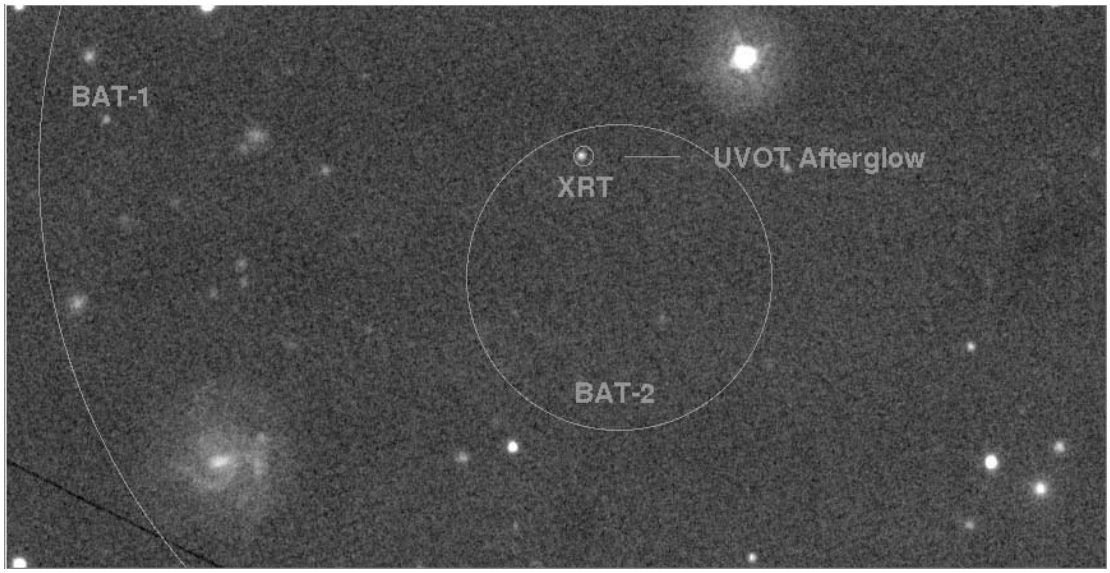

FIG. 1.—*Swift* UVOT *V*-filter image of the field around GRB 050603 with the BAT and XRT error circles superimposed. Positions are given in Table 2. BAT-1 refers to the on-board processed position and error circle and BAT-2 to the error circle from the data processed on the ground. [*See the electronic edition of the Journal for a color version of this figure.*]

converted into an unabsorbed flux by an energy conversion factor (ECF) using a power-law fit with the absorption column density fixed to the Galactic value (1.2×10^{20} cm^{-2}; Dickey & Lockman 1990). Only one ECF with ECF $= 3.76 \times 10^{-11}$ ergs s^{-1} cm^{-2} count^{-1} was applied for the whole light curve. As shown in § 3.3.2, there is no obvious change of the spectral parameters between early and later observations.

3. RESULTS

3.1. *Positions*

All positions given for GRB 050603 are listed in Table 2. Figure 1 displays the UVOT *V*-filter image of the GRB 050603 field with the BAT and XRT error circles superimposed, as given in Table 2. The XRT position given in Table 2 is corrected for the XRT boresight offset (Moretti et al. 2005) and differs slightly from the positions given by Grupe et al. (2005) and Racusin et al. (2005). This new XRT position is in excellent agreement with the UVOT, optical, and radio positions (Brown et al. 2005; Berger & McWilliam 2005; Cameron 2005).

3.2. *BAT*

The BAT mask-weighted light curve (Fig. 2) shows three fast-rise exponential-decay–like spikes with peaks at 2.7 and 0.85 s before the trigger and 0.15 s afterward. Each spike had a width of 0.6 s FWHM. The left panel of Figure 2 displays the light curve of the whole 15–350 keV energy band. The right panel shows the light curve split into four energy bands: 15–25, 25–50, 50–100, and 100–350 keV. The BAT light curve shows a harder spectrum during the spikes than the BAT observation after the spikes (Fig. 3).

The time-averaged spectrum between $T_0 - 3$ s and $T_0 + 18$ s in the 15–150 keV band shown in Figure 4 is well fitted by a single power law with an energy spectral slope $\beta_\gamma = 0.17^{+0.07}_{-0.08}$ ($\chi^2/\nu = 51/57$). The spectrum is background-subtracted. It has the standard 80 channel BAT energy binning.

GRB 050603 had $T_{90} = 12 \pm 2$ s that classifies it as a long burst. The fluence in the observed 15–150 keV band was $(7.6 \pm 0.3) \times 10^{-6}$ ergs cm^{-2}. Based on the redshift $z = 2.812$ (Berger & Becker 2005), the *k*-corrected rest-frame 100–500 keV and

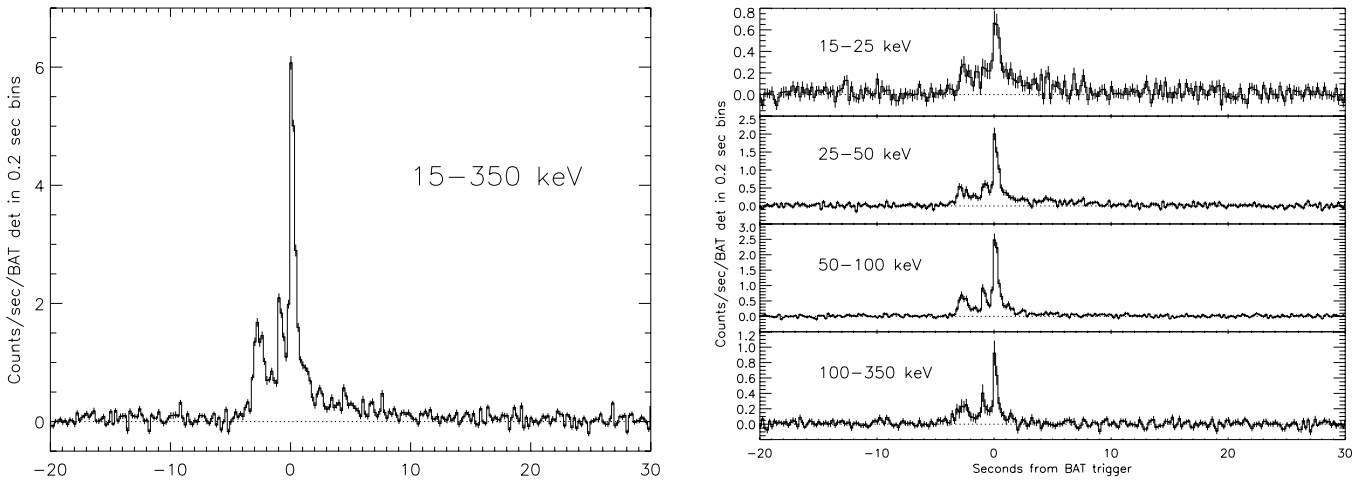

FIG. 2.—*Swift* BAT light curves. The left panel shows the light curve in the energy range 15–350 keV, and the right panel shows the light curve split into four subranges (see text).

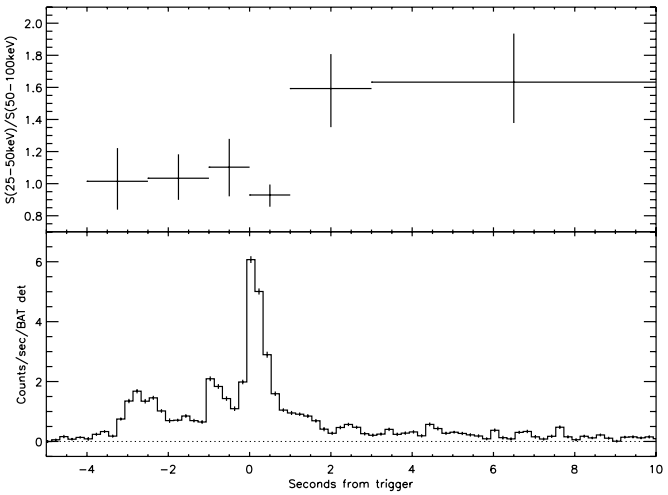

FIG. 3.—*Swift* BAT color ratio (*top*) and light curve (*bottom*).

20 keV–2 MeV total isotropic equivalent energies $E_{\gamma,\mathrm{iso}} = 3.2 \times 10^{53}$ and 1.26×10^{54} ergs, respectively, are some of the largest measured among all GRBs detected by *Swift* (Nousek et al. 2006). The total energies are comparable to other high-energetic pre-*Swift* bursts such as GRB 990123 (Briggs et al. 1999; Corsi et al. 2005), GRB 000131 (Andersen et al. 2000), or GRB 010222 (in't Zand et al. 2001).

3.3. *XRT Data*

3.3.1. *XRT Light Curve*

Figure 5 displays the 0.3–10 keV flux X-ray light curve of GRB 050603. The initial count rate at the beginning of the XRT observation was 0.06 counts s^{-1}, which converts to a 0.3–10.0 keV unabsorbed flux $F_X = 3 \times 10^{-12}$ ergs s^{-1} cm^{-2}. The 2.0–10.0 keV unabsorbed flux was $F_X = 2 \times 10^{-12}$ ergs s^{-1} cm^{-2}. The count rate was low enough that the data are not affected by pileup. The decay slope, derived from the 0.3–10.0 keV flux light curve shown in Figure 5, is unusually steep with $\alpha = 1.76^{+0.15}_{-0.07}$. This makes GRB 050603 a relatively rapidly fading afterglow in its late phase (Nousek et al. 2006). The data are consistent with one simple power law throughout the observation with a $\chi^2/\nu = 14.3/17$.

Just before the detection of GRB 050603 the XRT MOS CCD was hit by a micrometeorite that caused severe damage to columns 294 and 320. These columns (and several adjacent ones) have been disabled on board and are not usable. If the point-spread function of a source overlaps these bad columns, the measured flux can be incorrect. Since the source position on the detector changes with each orbit, this can lead to errors in the light curve. We have verified that the GRB was not positioned on the bad columns during this observation.

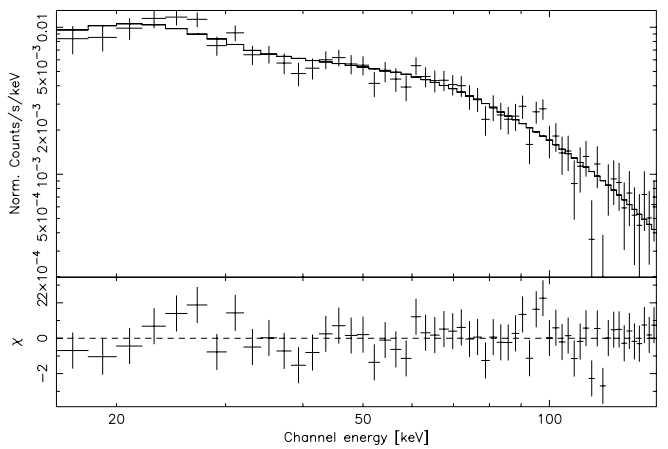

FIG. 4.—*Swift* BAT 15–150 keV spectrum.

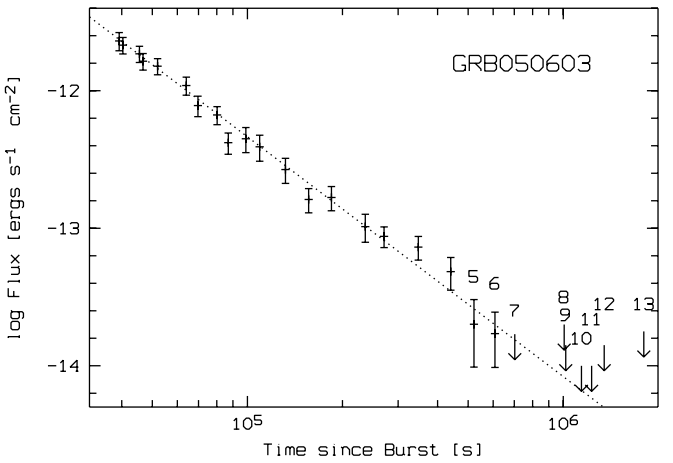

FIG. 5.—*Swift* XRT 0.3–10.0 keV unabsorbed flux light curve of GRB 050603 fitted in XSPEC by a single power law with $\alpha_3 = 1.76 \pm 0.07$. The downward arrows represent 3 σ upper limits. Numbers 5–13 refer to the segments as given in Table 1.

3.3.2. *X-Ray Spectral Analysis*

Table 3 lists the results of the spectral analysis of the XRT data. A simple power-law model with Galactic absorption fits the spectra well for the segment 001 and 002 (Table 1) data, resulting in X-ray energy spectral slopes $\beta_X = 0.80 \pm 0.17$ and 0.62 ± 0.13 for segments 001 and 002, respectively. The simultaneous fit to the segment 001 and 002 data is shown in Figure 6. The energy ranges of the two spectra are different due to the S/N and the binning of the channels using `grppha`. This fit results in an X-ray spectra slope $\beta_X = 0.71 \pm 0.10$. In all cases, no additional intrinsic absorption is required. Leaving the absorption column density as a free parameter results in an absorption column density that is significantly below the Galactic value. As shown in Figure 6 there are some apparent residuals around 0.5 and 2.0 keV. These features are due to systematic errors in the still ongoing calibration of the auxiliary response file (see the XRT calibration document XRT-OAB-CAL-ARF-v3[9] and Romano et al. 2005).

3.4. *UVOT*

The *V* magnitudes for GRB 050603 are listed in Table 4, and the *V*-band light curve is shown in Figure 7. The first measurement, $V = 18.2$ at 9.5 hr after the burst, is brighter than any

[9] The calibration document XRT-OAB-CAL-ARF-v3 can be found at http://swift.gsfc.nasa.gov/docs/heasarc/caldb/swift/docs/xrt/index.html.

TABLE 3

SPECTRAL ANALYSIS OF GRB 050603 WITH A POWER-LAW FIT WITH THE COLUMN DENSITY FIXED AT THE GALACTIC VALUE (1.19×10^{20} cm^{-2}; DICKEY & LOCKMAN 1990)

Segment	β_X	χ^2/ν
001	0.80 ± 0.17	13.5/13
002	0.62 ± 0.13	24.3/22
001 + 002	0.71 ± 0.10	39.2/36

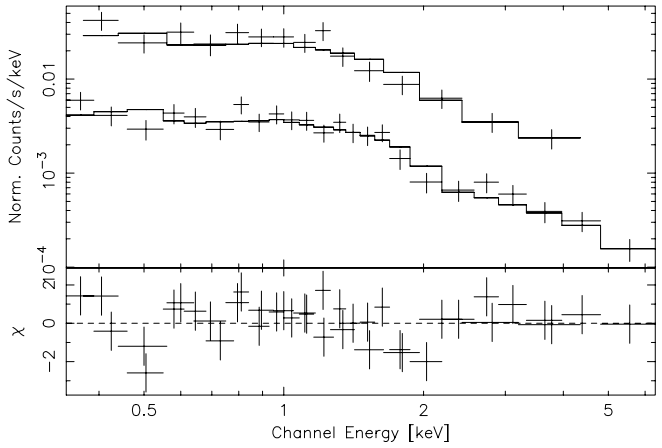

FIG. 6.—X-ray spectra of the observation segments 001 (*top*) and 002 (*bottom*; see Table 1) of GRB 050603 fitted by a single power law (see Table 3). The residuals at 0.5 and 2 keV are caused by systematic errors in the auxiliary response file calibration (§ 3.3.2).

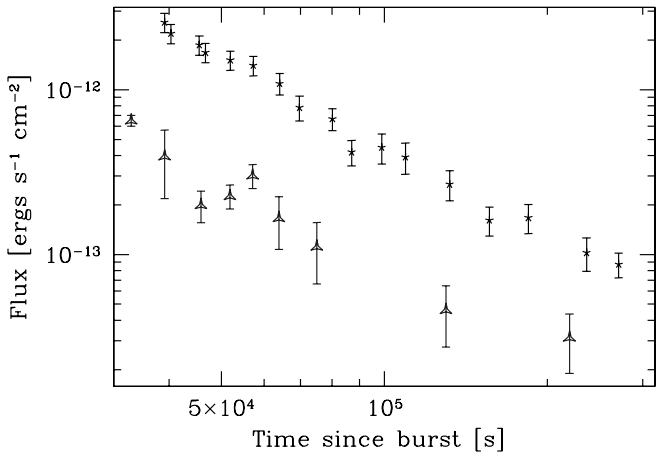

FIG. 7.—Combined XRT and UVOT *V*-filter light curves. The UVOT *V* fluxes were multiplied by a factor of 10^6 in order to plot them together with the XRT data. The XRT data are displayed as crosses and the UVOT *V*-band data as triangles. [*See the electronic edition of the Journal for a color version of this figure.*]

other optical *Swift* afterglow at the same time, many of which are not optically detected at all (see, e.g., Roming et al. 2005b), and is among the brightest of all optical afterglows with the exception of GRB 030329 (see, e.g., Berger et al. 2005). The X-ray and optical decay slopes are similar, with the UVOT points decaying with a power-law slope of 1.8 ± 0.2 with $\chi^2/\nu = 18/7$. There is no indication of a break near 12 hr as suggested by Berger & Becker (2005), although the errors and wide temporal sampling do not allow a definitive statement. The steepness of the decay indicates that the break may have already occurred before our observations began, which would put a putative break at less than $T + 9$ hr postburst.

The large value of χ^2/ν indicates that the deviations from the simple power law may be real, although the largest deviations are only 2 σ. Li et al. (2006), in an independent analysis of the UVOT data, also concluded that this afterglow exhibited real fluctuations from a power-law decay. The power-law decay reported by Li et al. (2006) is 1.86 ± 0.06, which is consistent with our results and also in agreement with that seen in the X-rays.

3.5. *Other Wavelengths*

GRB 050603 was the target of several ground-based observations at radio and optical wavelengths. Cameron (2005) reported the Very Large Array (VLA) position at 8.46 GHz as listed in Table 2. The flux density was 262 ± 41 μJy at 8.4 hr after the burst. The afterglow was also observed by SCUBA at 450 and 850 μm at 11.2 and 13.3 hr after the burst, respectively. Barnard et al. (2005) reported a 1.2 σ detection with a flux density of 2.408 ± 1.973 mJy at 450 μm, but no detection at 850μm.

Berger & McWilliam (2005) reported an *R*-band detection of the afterglow with the 2.5 m du Pont telescope at Las Campanas Observatory 3.4 hr after the burst with $R = 16.5$ mag. The optical position is given in Table 2. Berger & Becker (2005) measured the redshift of the afterglow as $z = 2.821$ based on a single emission line that was interpreted as Lyα. This observation was performed with the Magellan/Baade telescope 2.13 days after the burst.

GRB 050603 was also detected by the IBIS instrument on board *INTEGRAL* in the 40–300 keV energy range (Gotz & Mereghetti 2005). However, because the burst was outside the field of view, it could not be localized. The duration of the burst seen by IBIS agreed with the results from the BAT. Golenetskii et al. (2005) reported the detection of GRB 050603 by *Konus-Wind* in the observed 20 keV–3 MeV range. Its fluence in this energy band was $(3.41 \pm 0.06) \times 10^{-5}$ ergs cm^{-2}, with a duration of 6 s and an observed $E_{\rm peak} = 349 \pm 28$ keV.

TABLE 4
V MAGNITUDES GRB 050603 FROM THE UVOT OBSERVATIONS

$T_{\rm afterburst}$[a] (s)	$T_{\rm exp}$ (s)	*V* Mag	*V* Error
34093	1298	18.19	0.08
39276	110	18.73	0.40
45864	1772	19.47	0.21
51840	2104	19.33	0.17
57096	1200	19.02	0.17
63900	1205	19.67	0.33
75024	2056	20.1	0.37
129996	10458	21.06	0.37
219708	10945	21.48	0.36

[a] The times after the burst mark the middle of the time bin.

4. DISCUSSION

GRB 050603 was a particularly bright and energetic burst. The 15–150 keV fluence of 7.6×10^{-6} ergs cm^{-2} places it among the top 10% of *Swift* bursts. The isotropic energy of 1.26×10^{54} ergs makes it one of the most energetic bursts ever detected. Combined with the rest-frame $E_{\rm peak} = 1.3$ MeV, GRB 050603 is consistent with the Amati relation (Amati et al. 2002).

With an optical magnitude of $V = 18.2$ 9.5 hr after the burst, GRB 050603 was also the brightest optical afterglow seen so far by *Swift* at this late time after the burst. The only burst that had a comparable magnitude ($V = 18.9$) at 10 hr after the burst was GRB 050525 (Blustin et al. 2006). All other bursts were far below this magnitude at this time after the burst. In X-rays, however, the afterglow of GRB 050603 was not the brightest one among other *Swift* bursts observed at similar times after the trigger.

The X-ray afterglow of GRB 050603 decayed with a rather steep slope of $\alpha = 1.76 \pm 0.07$, compared with the mean decay slope of $\alpha = 1.34 \pm 0.32$ for 27 bursts listed in Nousek et al. (2006). This is intermediate between the slopes of $\sim 1.3 \pm 0.1$ obtained from *Chandra* grating observations, *XMM-Newton* observations,

and the *BeppoSAX* afterglows discussed in Gendre et al. (2006), but is somewhat shallower than the mean decay slope of $\alpha_X = 2.0 \pm 0.3$ from their survey of *Chandra* imaging afterglow observations. It is also intermediate between the expectations for the "normal" afterglow slope following the end of energy injection by the central engine, and the steeper slope expected following the end of energy injection by the central engine. We note, however, that the decay slope in the *V*-band filter ($\alpha = 1.8 \pm 0.2$) is consistent with the X-ray decay slope, consistent with the typical signature of an afterglow after the jet break (Sari et al. 1999). This suggests the possibility that GRB 050603 had an early jet break before 2.9 hr (rest frame) after the burst. If we assume that the jet break happened before the start of the UVOT and XRT observations, we can use the dependence of jet angle on break time (Sari et al. 1999; Frail et al. 2001) to place a limit on the jet opening angle of $\Theta_j < 1.^\circ3$, where we have used $E_{\rm iso} = 1.26 \times 10^{54}$ ergs and we assumed the density of the circumburst matter is 0.1 cm^{-3}. We note that Bloom et al. (2003) argue for a larger typical circumburst density of 10 cm^{-3}, which would imply a slightly larger jet angle limit of $2.^\circ3$.

In order to check the jet interpretation, we compare the observed $\alpha_X = 1.76^{+0.15}_{-0.07}$ and $\beta_X = 0.71 \pm 0.10$ to the prediction of the jet model. For the familiar case of $p > 2$ (where p is the electron spectral index), one requires that $\alpha_X - 2\beta_X = 0$ ($\nu > \nu_c$) or $\alpha_X - 2\beta_X = 1$ ($\nu_m < \nu < \nu_c$), where ν_m is the typical synchrotron frequency (injection frequency) and ν_c is the cooling frequency (Rhoads 1999). In this case, we have $\alpha_X - 2\beta_X = 0.34^{+0.18}_{-0.12}$. Both cases are inconsistent with the data at the $>2.8\,\sigma$ level. We therefore consider the case of $1 < p < 2$ (Dai & Cheng 2001). For $\nu > \nu_c$, this case has $2\alpha_X - \beta_X = 3$, while the data have $2\alpha_X - \beta_X = 2.81^{+0.32}_{-0.12}$, in good agreement with theory. In this regime the electron index is $p = 2\beta_X = 1.4 \pm 0.2$. This case also has $\alpha_o = \alpha_X$ as long as the self-absorption frequency is below the optical band, in agreement with the observations. In this case, we expect $\beta_o = \beta_X$ if the optical band is above the cooling frequency, or $\beta_o = 0.2 \pm 0.1$ if the optical band is between the injection frequency and the cooling frequency; however, with only *V*-band data we cannot constrain β_o directly. The observed spectral index between the X-ray and optical bands is $\beta_{\rm ox} = 0.04$.[10] These spectral slopes suggest that there is a break in the spectrum between the optical and X-rays, suggesting that the optical band is between the injection and cooling frequencies. We therefore conclude that the jet interpretation fits these data, provided that there is a flat electron energy spectrum $p = 1.4$ (Dai & Cheng 2001). We note, however, that this interpretation is at odds with the expectations of Liang & Zhang (2005), who find the relation $E_{\gamma,{\rm iso},52} = 0.85(E_{\rm peak}/100\ {\rm keV})^{1.94} t^{-1.34}$, which predicts a jet break in the optical light curve at 1 day after the burst in the rest frame, or 3.8 days in the observed frame.

We would like to thank the anonymous referee for valuable comments and suggestions that improved the paper. We would also like to thank Vicki Barnard and Brian Cameron for their information on the SCUBA and VLA observations. We made use of data obtained through the High Energy Astrophysics Science Archive Research Center Online Service, provided by the NASA Goddard Space Flight Center. This work has been supported by NASA contract NAS5-00136, SAO grant GO5-6076 BASIC, and NASA grant NNG05GF43G.

[10] Here we define the optical to X-ray spectral slope $\beta_{\rm ox} = \log(5460\ \text{Å} \times f_{5460\ \text{Å}}) - \log(1\ {\rm keV} \times f_{1\ {\rm keV}})$.

REFERENCES

Amati, L., et al. 2002, A&A, 390, 81
Andersen, M. I., et al. 2000, A&A, 364, L54
Barnard, V., Schieven, G., Tilanus, R., Lundin, E., & Ivison, R. 2005, GCN Circ. 3515, http://gcn.gsfc.nasa.gov/gcn/gcn3/3515.gcn3
Barthelmy, S. D. 2005, Space Sci. Rev., 120, 143
Berger, E. 2005, GCN Circ. 3517, http://gcn.gsfc.nasa.gov/gcn/gcn3/3517.gcn3
Berger, E., & Becker, G. 2005, GCN Circ. 3520, http://gcn.gsfc.nasa.gov/gcn/gcn3/3520.gcn3
Berger, E., & McWilliam, A. 2005, GCN Circ. 3511, http://gcn.gsfc.nasa.gov/gcn/gcn3/3511.gcn3
Berger, E., et al. 2005, ApJ, 629, 328
Bloom, J. S., Frail, D. A., & Kulkarni, S. R. 2003, ApJ, 594, 674
Blustin, A. J., et al. 2006, ApJ, 637, 901
Briggs, M. S., et al. 1999, ApJ, 524, 82
Brown, P., et al. 2005, GCN Circ. 3516, http://gcn.gsfc.nasa.gov/gcn/gcn3/3516.gcn3
Burrows, D. N., et al. 2005, Space Sci. Rev., 120, 165
Cameron, P. B. 2005, GCN Circ. 3513, http://gcn.gsfc.nasa.gov/gcn/gcn3/3513.gcn3
Corsi, A., et al. 2005, A&A, 438, 829
Dai, Z. G., & Cheng, K. S. 2001, ApJ, 558, L109
Dickey, J. M., & Lockman, F. J. 1990, ARA&A, 28, 215
Eichler, D., Livio, M., Piran, T., & Schramm, D. N. 1989, Nature, 340, 126
Fenimore, E., et al. 2005, GCN Circ. 3512, http://gcn.gsfc.nasa.gov/gcn/gcn3/3512.gcn3
Frail, D. A., et al. 2001, ApJ, 562, L55
Gehrels, N., et al. 2004, ApJ, 611, 1005
Gendre, B., Corsi, A., & Piro, L. 2006, A&A, in press (astro-ph/0507710)
Golenetskii, S., Aptekar, R., Mazets, E., Pal'shin, V., Frederiks, D., & Cline, T. 2005, GCN Circ. 3518, http://gcn.gsfc.nasa.gov/gcn/gcn3/3512.gcn3
Gotz, D., & Mereghetti, S. 2005, GCN Circ. 3510, http://gcn.gsfc.nasa.gov/gcn/gcn3/3512.gcn3
Grupe, D., Retter, A., Burrows, D. N., Kennea, J. A., & Gehrels, N. 2005, GCN Circ. 3519, http://gcn.gsfc.nasa.gov/gcn/gcn3/3512.gcn3
Hill, J. E., et al. 2004, Proc. SPIE, 5165, 217
Hogg, D. 1999, preprint (astro-ph/9905116)
in't Zand, J. J. M., et al. 2001, ApJ, 559, 710
Kouveliotou, C., et al. 1993, ApJ, 413, L101
Li, W., Jha, S., Filippenko, A. V., Bloom, J. S., Pooley, D., Foley, J., & Perley, D. A. 2006, PASP, 118, 37
Liang, E., & Zhang, B. 2005, ApJ, 633, 611
Mason, K. O., et al. 2001, A&A, 365, L36
Mészáros, P., & Rees, M. J. 1997, ApJ, 476, 232
Moretti, A., et al. 2006, A&A, 448, L9
Nousek, J., et al. 2006, ApJ, 642, 389
Paczyński, B. 1991, Acta Astron., 41, 257
Racusin, J. L., Burrows, D. N., Kennea, J. A., Retter, A., Pagani, C., Wells, A., & Gehrels, N. 2005, GCN Circ. 3514, http://gcn.gsfc.nasa.gov/gcn/gcn3/3514.gcn3
Retter, A., Parsons, A., Gehrels, N., Gronwall, C., Markwardt, C. B., & Palmer, D. 2005, GCN Circ. 3509, http://gcn.gsfc.nasa.gov/gcn/gcn3/3509.gcn3
Rhoads, J. 1999, ApJ, 525, 737
Romano, P., et al. 2005, Proc. SPIE, 5898, 369
Roming, P. W. A., et al. 2005a, Space Sci. Rev., 120, 95
———. 2005b, ApJ, submitted (astro-ph/0509273)
Sari, R., Piran, T., & Halpern, J. P. 1999, ApJ, 519, L17
Sari, R., Piran, T., & Narayan, R. 1998, ApJ, 497, L17
Turner, M. J. L., et al. 2001, A&A, 365, L27
Woosley, S. E. 1993, ApJ, 405, 273
Zhang, B., Fan, Y. Z., Dyks, J., Kobayashi, S., Mészáros, P., Burrows, B. N., Nousek, J. A., & Gehrels, N. 2006, ApJ, 642, 354
Zhang, B., & Mészáros, P. 2004, Int. J. Mod. Phys. A, 19, 2385